Supplemental Figures and Legends

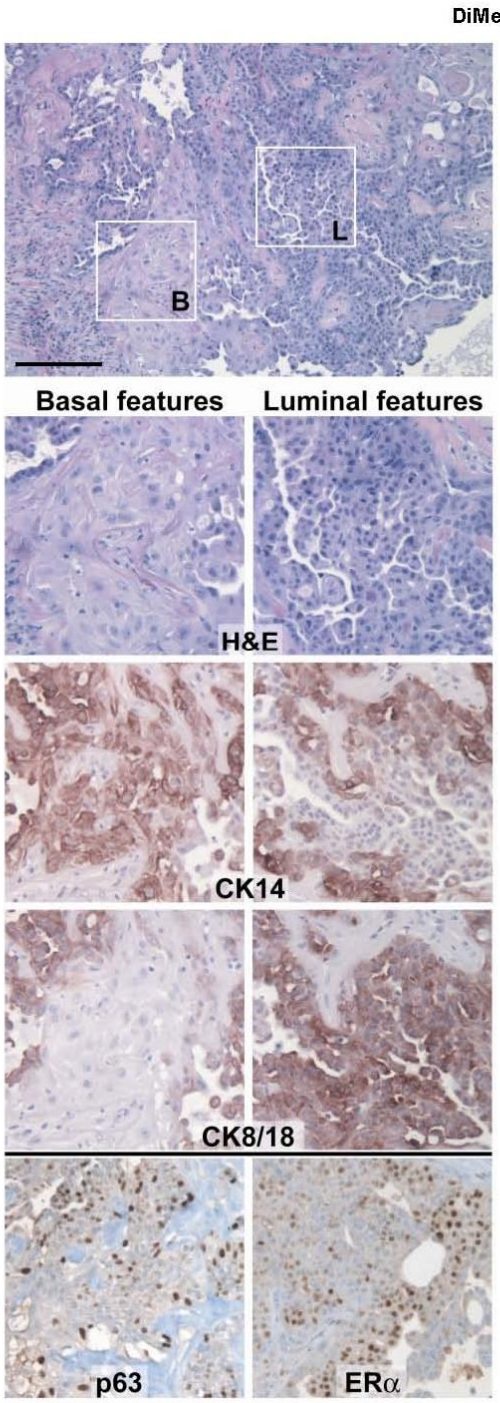

Supplemental Figure 1. Tumors generated from unsorted cells have a mixed phenotype (related to Figure 1) Representative H&E stained tumor section at 100X magnification to show the inter-tumor heterogeneity including areas squamous and papillary growth (scale bar = 200μm). Areas highlighted are shown at higher magnification to illustrate basal-type and luminal-type characteristics and immunoreactivity for CK14 and p63, as well as areas of luminal phenotype that have a papillary growth pattern and reactivity for CK8/18 and ER. Some areas appear to be reactive for markers of both tumor types.

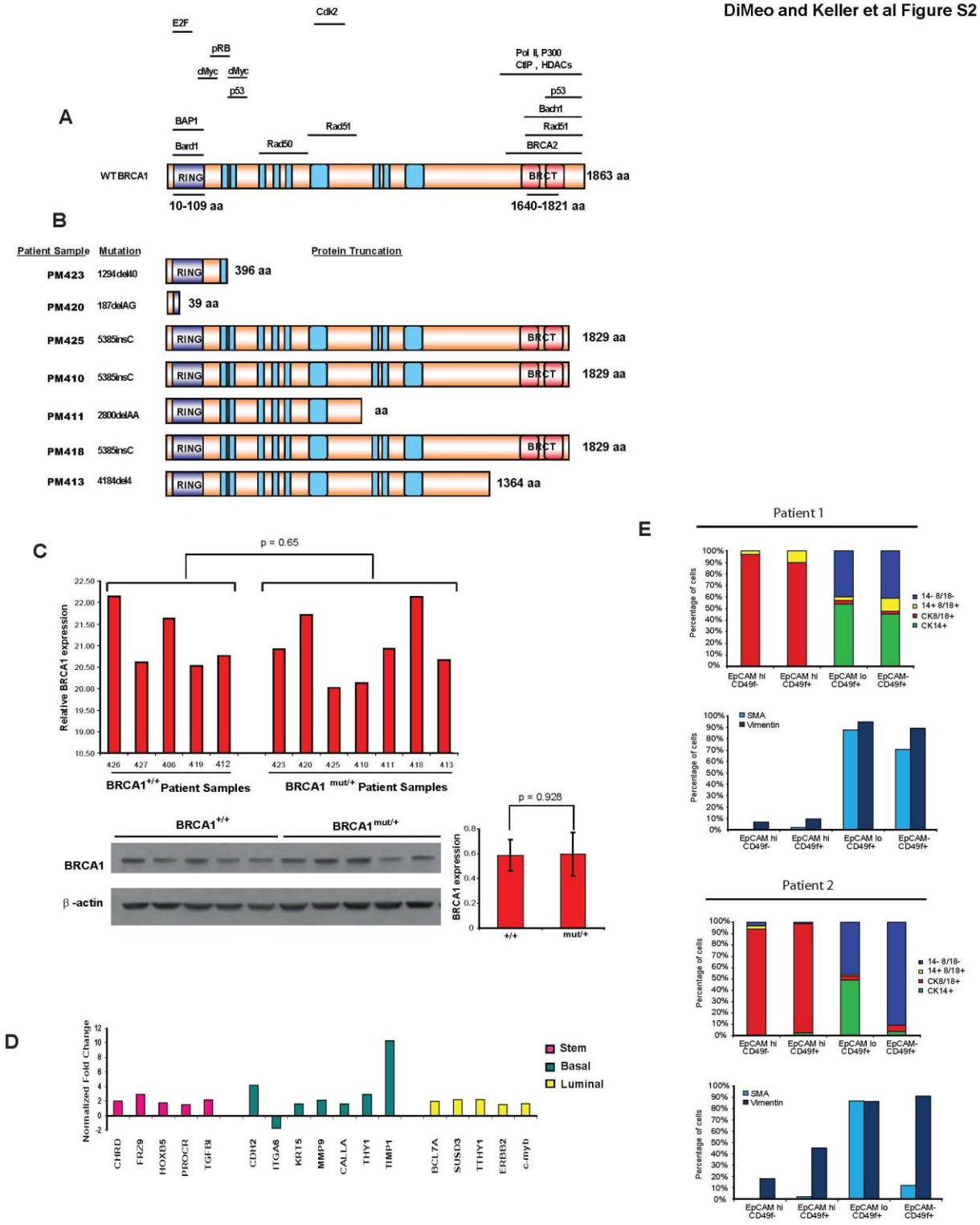

Supplemental Figure 2. Characterization of BRCA1 mutations, expression and cell types (related to Figure 3) **(A)** Schematic diagram of WT BRCA1 protein including domains and known interacting proteins. **(B)** Schematic diagram of deleterious BRCA1 mutants found in the patient samples used in this study. **(C)** qRT-PCR and western blot analysis of BRCA1 expression in

BRCA1$^{+/+}$ and BRCA1$^{mut/+}$ breast epithelial cells used in this study. **(D)** Array qRT-PCR against a panel of 86 genes expressed in breast luminal, basal and stem cells was performed on BRCA1$^{+/+}$ and BRCA1$^{mut/+}$ breast epithelial cells. Only genes that were differentially expressed 1.5-fold or greater between *BRCA1*$^{+/+}$ and *BRCA1*$^{mut/+}$ cells are shown. Genes known to be expressed in basal cells (teal), luminal cells (yellow) and stem cells (pink) were differentially expressed. **(E)** Cytokeratin (CK) 18, 14, smooth muscle actin (αSMA) and vimentin quantification of immunofluorescence staining on cytospun sorted populations of cells indicates luminal and basal/myoepithelial cell enrichment.

DiMeo and Keller et al Figure S3

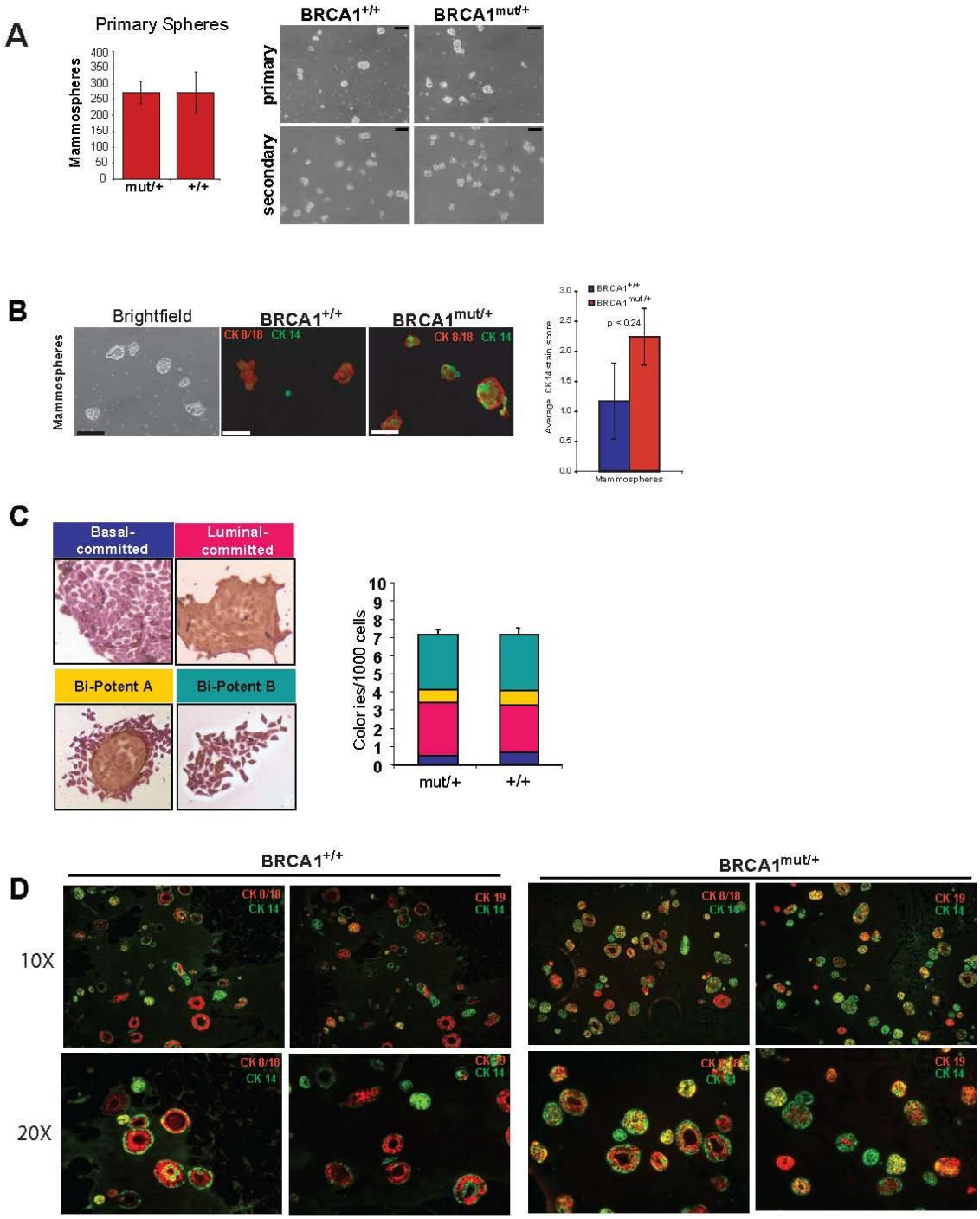

Supplemental Figure 3. Molecular and cellular characterization of BRCA1$^{mut/+}$ cells
(related to Figure 3) **(A)** Human mammary epithelial cells were grown in non-adherent conditions to promote the formation of mammospheres (scale bar = 100 μm). Quantification of the average number of mammospheres >30 μm from 4 different *BRCA1*$^{+/+}$ patient samples and 4 different *BRCA1*$^{mut/+}$ patient samples using the Multisizer 3 COULTER COUNTER.. Error bars are +/- SD**.** **(B)** Cytospun spheres were stained for CK 8/18 (red) and 14 (green)(scale bar = 100 μm). CK14 content in spheres was scored as described in methods. At least 30 spheres were scored for each patient sample. The average scores from 3 *BRCA1*$^{+/+}$ and *BRCA1*$^{mut/+}$ patient samples are shown in the graph. Error bars are +/- SEM and p-values were calculated by two-tailed t-test. **(C)** Breast epithelial cells produced 4 types of adherent colonies: (1) colonies exclusively positive for the luminal-associated keratins 8/18 derived from luminal-committed progenitor cells, (2) colonies exclusively positive for the basal-associated keratin 14 derived from basal-committed progenitor cells, and (3,4) two distinct types of bipotent progenitor colonies; one type of bipotent colony contains a central core of cells expressing luminal keratin 8/18-positive cells surrounded by keratin 14-positive basal-like cells (bi-potent A) while the other type of bipotent colony is composed of double-positive cells expressing both keratin 14 and keratin 8/18 as well as cells positive for only keratin 8/18 or 14 (bi-potent B). Middle graph: quantification of the total number and type of colonies formed under adherent conditions with 4 patients each, *BRCA1*$^{mut/+}$ and *BRCA1*$^{+/+}$. Right graph: breast epithelial cells also produce small (~30-50μm) suspension spheres when grown under adherent conditions. No difference in the number of suspension spheres from BRCA1$^{+/+}$ or BRCA1$^{mut/+}$ breast epithelium (n = 4 patient samples from each genotype). **(D)** Acinar structures from patient-derived *BRCA1*$^{+/+}$ and *BRCA1*$^{mut/+}$ patient cells grown in the HIM model. Tissue outgrowths were double stained for CK14 and CK8/18 or CK19. The staining was characterized as mature (CK14+ basal/ME layer and CK8/18 and/or 19+ luminal layer), immature (CK14+ basal/ME layer and CK14 and CK8/19 and/or 19+ luminal layer) or other (CK14 only, CK8/18/19 only etc.).

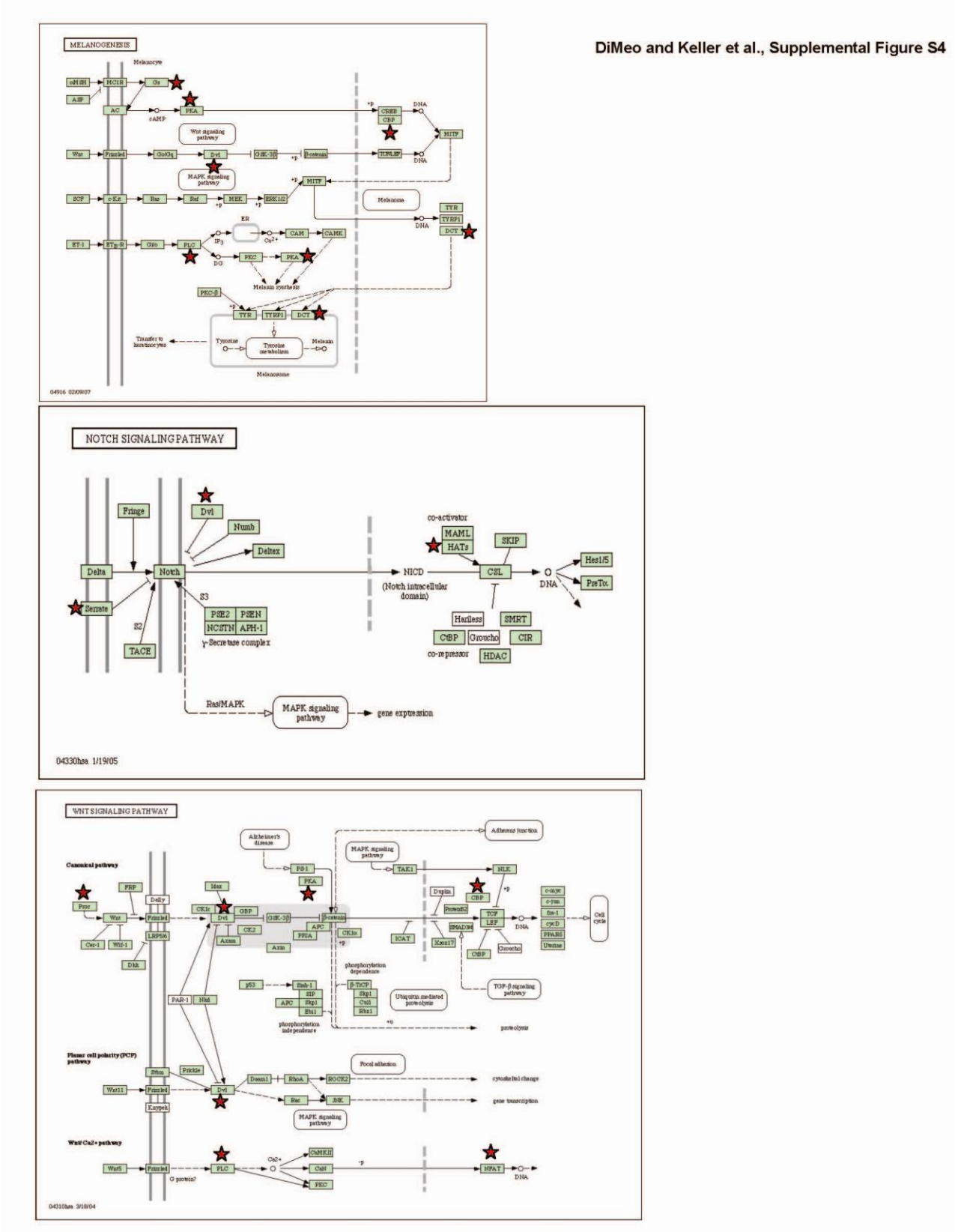

Supplemental Figure 4. Pathway analysis of genes identified in BRCA1 $^{mut/+}$ signature (related to Figure 5) Pathways shown are based on known Kegg pathways obtained from DAVID functional annotation and gene classification Bioinformatics Resources 2008. Red stars represent genes that are up-regulated in breast epithelial cells of BRCA1-mutation carriers.

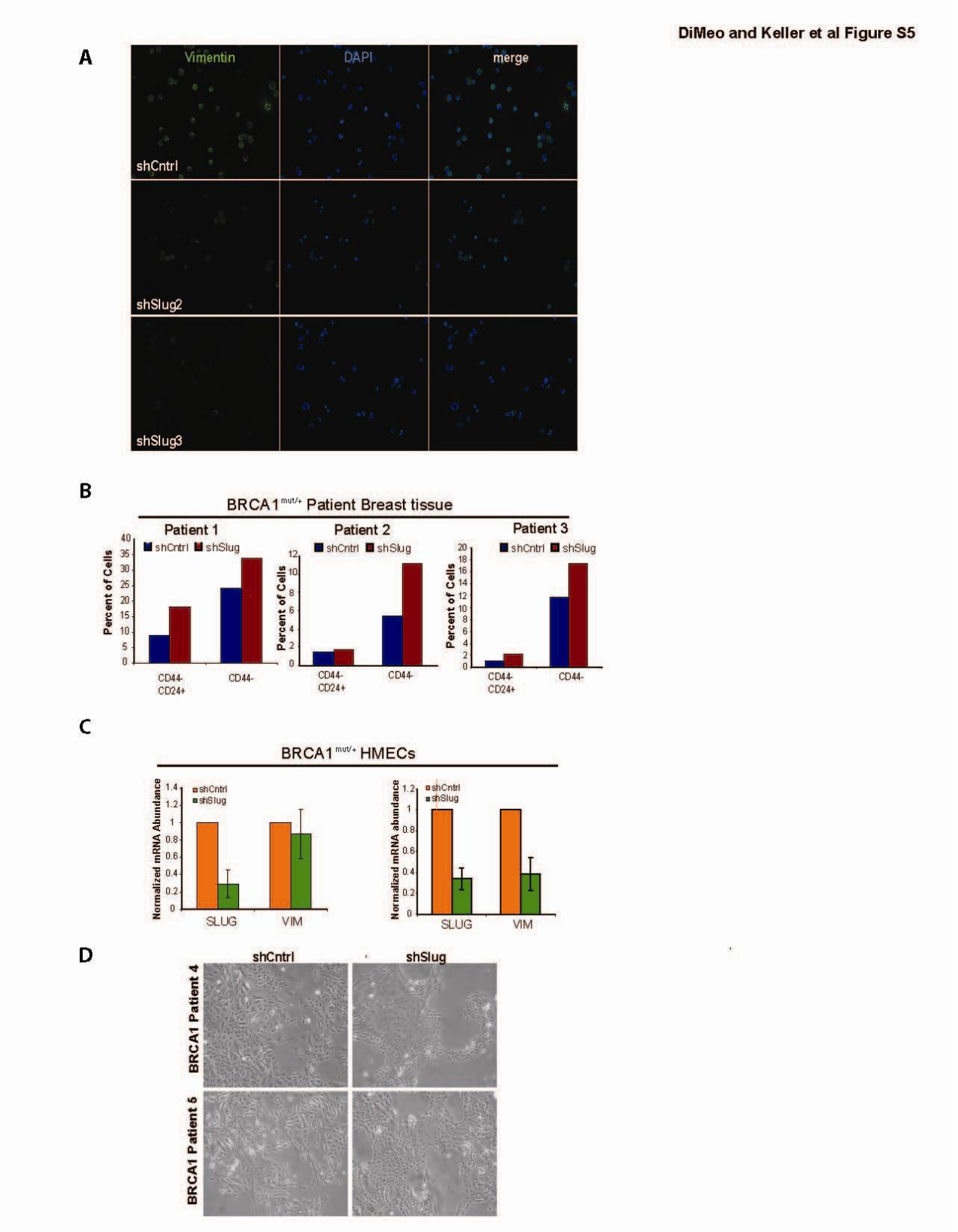

Supplemental Figure 5. Slug inhibition decreases basal differentiation

(related to Figure 5) **(A)** Vimentin immunofluorescence staining of patient-derived BRCA1$^{mut/+}$ cells infected with lentiviruses targeting Slug (shSlug2 and shSlug3) or a scrambled sequence (shCntrl). **(B)** Flow cytometry analysis of CD44 and CD24 expression in patient-derived

BRCA1$^{mut/+}$ breast epithelial cells following Slug knockdown. **(C)** QRT-PCR of SLUG and vimentin mRNA expression in two different immortalized BRCA1$^{mut/+}$ breast epithelial cell lines following Slug knockdown. **(D)** Brightfield image of two different immortalized BRCA1$^{mut/+}$ breast epithelial cell lines following Slug knockdown. Note the increased epithelial morphology in shSlug cells.

DiMeo and Keller et al Figure S6

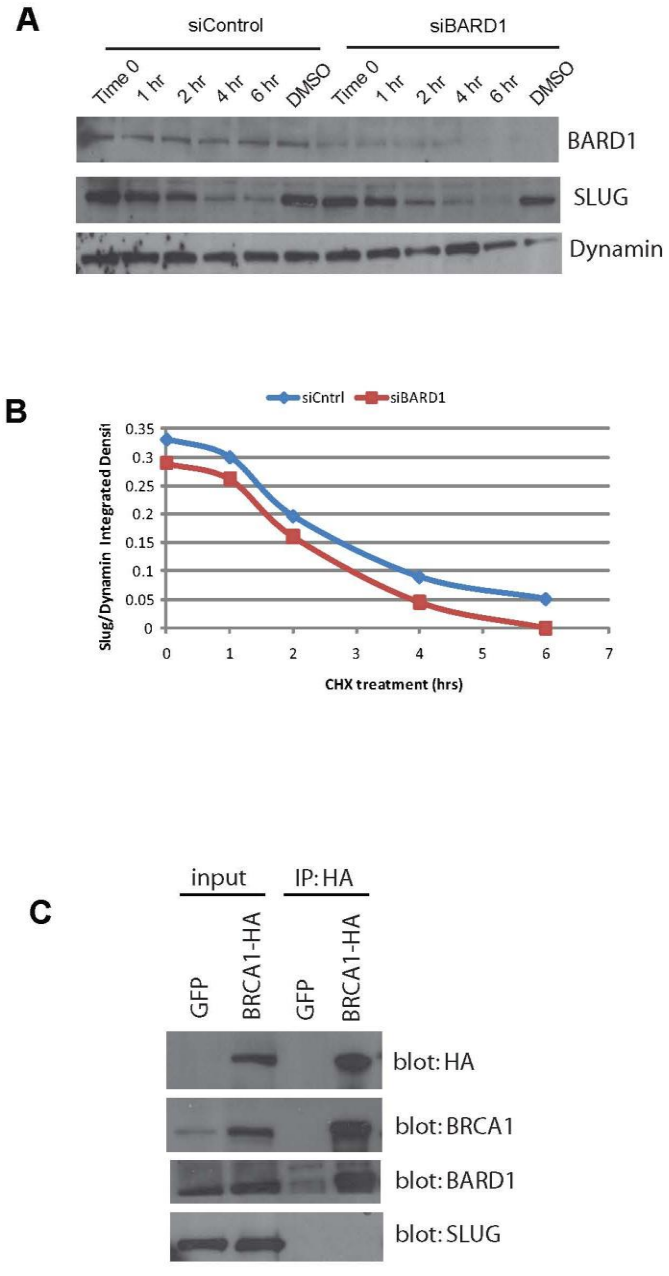

Supplemental Figure 6. BRCA1/BARD1 and Slug do not interact
(related to Figure 6) **(A, B)** *BRCA1*$^{+/+}$ (MCF10A) cells were transfected with si*BARD1 or siControl* and treated with cycloheximide (CHX) to prevent further protein synthesis at indicated time intervals. Western blot analysis demonstrates that Slug protein is turned over with similar kinetics in siControl MCF10A and siBARD1 MCF10A cells. **(C)** Protein lysates from 293T cells expressing GFP, HA-tagged full length BRCA1, or FLAG-tagged Slug were immunoprecipitated with antibodies directed at HA or FLAG, respectively. Co-IPs were blotted with antibodies directed against BARD1, BRCA1, Slug and HA as indicated.

DiMeo and Keller et al Figure S7

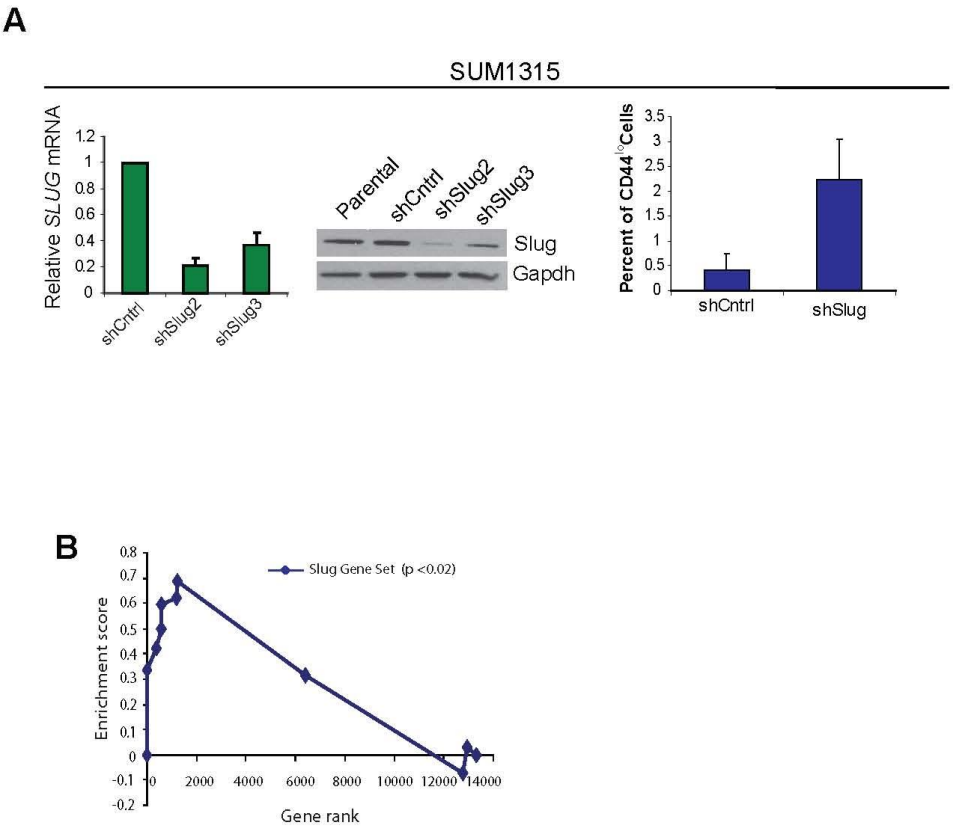

Supplemental Figure 7. Slug inhibition decreases basal tumor phenotype
(related to Figure 7) **(A)** qRT-PCR and Western blot analysis confirming Slug knockdown in SUM1315. Flow cytometry analysis of CD44 and CD24 expression in SUM1315 following Slug knockdown. **(B)** GSEA analysis indicates the Slug gene set is enriched in breast epithelial cells isolated from *BRCA1*$^{mut/+}$ patient samples.

Supplemental Experimental Details

BRCA1-mutation carrier tissues

All human breast tissue procurement for these experiments was obtained in compliance with the laws and institutional guidelines, as approved by the institutional IRB committee from Beth Israel Deaconess Medical Center (BIDMC) and Tufts University School of Medicine. Disease-free prophylactic mastectomy (n=31; 12 fresh, 19 formalin-fixed paraffin embedded) and tumor tissues (n=19) derived from women carrying a known deleterious *BRCA1* heterozygous mutation were obtained with patient consent from the Surgical Pathology files or immediately following prophylactic mastectomy surgery at BIDMC. Tissues in which BRCA1 mutation was confirmed but not known were submitted for sequence/genotyping at Myriad Genetic Laboratories. Non-*BRCA1* tumor tissues (n=20) were obtained from discarded material at Tufts Medical Center and non-cancerous breast tissue was obtained from patients undergoing elective reduction mammoplasty at Tufts Medical Center or BIDMC (n=38; 18 fresh, 24 formalin-fixed paraffin embedded). *BRCA1* mutation status and clinical information are listed in Table S1. The range of patient ages for fresh $BRCA1^{+/+}$ tissue used in this study was 30-54 with a median age of 40; the range of patient ages for fresh $BRCA1^{mut/+}$ tissue used in this study was 35-53 with a median age of 44. All disease-free breast tissues were verified by surgical pathologists prior to use in these studies.

Cell Lines and Tissue Culture

SUM cell lines were obtained from Dr. Stephen Ethier (Kramanos Institute, MI), while the MCF10A cell lines were purchased from ATCC. MCF10A cells were cultured in DMEM with 10% calf serum. SUM149PT cells were cultured in Ham's F12 with 5% calf serum, insulin (5 μg/mL), and hydrocortisone (1 μg/mL) while SUM1315MO2 were in Ham's F12 with 5% calf serum, insulin (5 μg/mL), and EGF (10 ng/mL). All cell lines were grown at 37ºC and 5% CO_2.

BRCA1$^{mut/+}$ HMECs were immortalized with the catalytic subunit of human telomerase as previously described (Elenbaas et al, 2000). BHME cells were cultured in MEGM (Lonza) supplemented with bovine pituitary extract (BPE), insulin (5 μg/mL), EGF (10 ng/mL) and hydrocortisone (1 μg/mL).

Lentiviral Constructs and virus production

Lentiviral constructs used for gene transduction into human mammary epithelial cells were created using standard cloning techniques into the self-inactivating CS-CG (Miyoshi et al., 1998) viral vector generously provided by Inder Verma (Salk Institute, La Jolla, CA). We obtained the pLENTI-*KRAS*^{G12V} and pLenti-CMV-*PIK3CA*-*myr*+CMV-*CCND1* from Min Wu (Aveo Pharmaceuticals, Cambridge, MA). A wild-type human *p53* cDNA clone was generously provided by Josh LaBaer (Harvard Institute of Proteomics, Harvard Medical School, Cambridge, MA). Site directed mutagenesis was employed to change amino acid residue 175 from R to H. The VSV-G-pseudotyped lentiviral vectors were generated by transient co-transfection of the vector construct with the VSV-G-expressing construct pCMV-VSV-G (Miyoshi et al., 1998) and the packaging construct pCMV ΔR8.2Δvpr (Miyoshi et al., 1998) generously provided by Inder Verma, into 293T cells with the FuGENE 6 transfection reagent (Roche). High-titer stocks of the virus were prepared by ultracentrifugation at 100,000 x g. Lentiviral shRNA constructs targeting Slug (Addgene plasmids 10904 and 10905) were prepared as previously described (Gupta et al., 2005).

Breast epithelial cell isolation and infection

Breast tissues were minced and enzymatically digested overnight with a mixture of collagenase and hyaluronidase as previously described (Kuperwasser et al., 2004; Proia and Kuperwasser, 2006). Digested cells were plated briefly in serum (1-2 hours) to deplete mammary fibroblasts from the organoid fraction of mammary fibroblasts. The organoids were dissociated to

a single cell suspension by trypsinization and filtered with a 40-μm filter (BD Biosciences) to remove residual clustered cells. Immediately after dissociation, cells were resuspended in 1 ml of MEGM medium (Lonza) containing 10^5 to10^7 cfu lentiviruses expressing the genes of interest and the cell/virus mixture was subjected to one round of spin infection in suspension at 1500 rpm for 90 minutes. The cell/virus mixture was incubated overnight at 37C following spin infection and infected cells were prepared for injection into cleared and humanized mammary fat pads. Time between cell dissociation, infection and injection was less than 24 hours.

Animals and Surgery

All animal procedures were conducted in accordance with a protocol approved by the Tufts University IACUC committee. A colony of immunocompromised NOD/SCID mice was maintained in house under aseptic sterile conditions. Mice were administered autoclaved food and water ad libitum. Surgeries were performed under sterile conditions, and animals received antibiotics in the drinking water up to two weeks after all surgical procedures.

Three-week-old female mice were anesthetized and the mammary epithelium was removed from the 4th inguinal mammary glands of NOD/SCID mice. Concurrently, mammary fat pads were humanized by the introduction of a 50:50 mixture (5×10^5 total cells per gland) of untreated human mammary fibroblasts overexpressing HGF (RMF-EG/HGF cells) and RMF-EG/HGF cells that had been treated with 2 mU/ml bleomycin sulfate (Calbiochem) for 30 min 18-24 hours prior to surgery. Two to four weeks post-humanization, viable GFP virus or oncogene virus-infected cells (100,000 per gland) were co-mixed with RMF-EG/HGF cells ($2.5x10^5$per gland) in a 1:1 mixture of collagen and matrigel (BD Biosciences) and injected into humanized fat pads as described previously (Kuperwasser et al., 2004; Proia and Kuperwasser, 2006).

Wholemount and Immunohistochemistry

GFP wholemount analysis was performed as previously described (Kuperwasser et al., 2004). Immunohistochemistry was performed on paraffin-embedded tissue sections with sodium citrate antigen retrieval, followed by visualization with the ABC Elite peroxidase kit and NovaRed substrate (Vector labs) for detection of αSMA (1:500, clone αsm-1), CK14 (1:500, clone LL002), CK8/18 1:500, clone DC-10), Vimentin (1:500, clone V9), CK19 (1:500, clone b170) (all, Vector Labs), TFF3 (Abnova, clone 3D9, 1:200)) and Slug (1:200, Cell Signaling). Staining for pan-cytokeratin (Ventana Medical Systems), p53 (Ventana Medical Systems), cyclin D1 (NeoMarkers), pAKT (Cell Signaling, 1:100), ER (Ventana Medical Systems), p63 (Ventana Medical Systems), and PR was performed by the Histology Special Procedures Laboratory at Tufts Medical Center.

IHC results were semi-quantitatively analyzed in a blinded fashion across multiple patient samples using the Allred scoring metric. For PR, Slug and TFF3, a 0-3 scale for staining intensity and a 0-5 scale for the percent cells stained was employed. The staining intensity and percent staining scores were added to obtain a total stain score for each lobule. An average total stain score over 5-25 different lobules or regions within the same tissue section were calculated for the staining for a particular patient sample. Statistical analysis was performed using the student's T-test across 10-25 different patient samples. For vimentin quantification, a modified metric was employed. A + to +++ score was employed for lobule staining. (+) exhibited weak staining and <10% positive cells with < 10% positive lobules positive. (++) exhibited moderate to strong intensity staining of cells with >10% but <50% positive cells and >10% positive lobules. (+++) exhibited strong intense staining of lobules with >50% cells and > 30% lobules staining positive. HIM tumor IHC results were quantitatively analyzed on the entire tissue section from 3-4 different tumors using Image J software.

RT-PCR analysis

RNA was extracted from the *KRAS/p53R175H/CCND1/PIK3CA* tumors and from cell lines with the RNAeasy Mini Kit (Qiagen). Standard RT-PCR to confirm expression of KRAS lentiviral construct-specific transcript, and quantitative real time PCR was used for detecting Slug, BRCA1, Snail, Twist, and Vimentin transcript in cell lines. The primer pairs were designed such that one primer is from the lentiviral vector, the other one is from the gene to be analyzed. In this way, only transcripts from the lentiviral constructs, but not normal human genomic locus, could be amplified. Primer sequences for KRAS (149bp):Forward 5'-TAGAGGATCCACTAGTACCACCATG-3' and Reverse 5'-GCTTCCTGTAGGAATCCTCTATTG-3'; GAPDH (185bp) Forward 5' GAGTCAACGGATTTGGTCGT 3' and Reverse 5' -GACAAGCTTCCCGTTCTCAG 3'; SLUG Forward 5', RNA was collected from cancer cell lines and cells post-siRNA knockdown and expression levels of SLUG and BRCA1 were analyzed. SLUG: Forward 5' GCATTTCTTCACTCCGAAGC and Reverse 5' TGAATTCCATGCTCTTGCAG 3'; BRCA1 Forward 5' GAAACCGTGCCAAAAGACTTC 3' Reverse 5' TCACAAGCAGCCAATTCAATGT 3'.

Mammospheres and Adherent colony forming assays

Viable cells dissociated from organoids derived from *BRCA1*$^{+/+}$ (n=4) and *BRCA1*$^{+/-}$ (n=4) patients were plated at 35,000 cells per well in 6-well plates for adherent colony growth in MEGM media (Lonza) or at 20,000 cells per ml in 6-well ultra-low attachment plates (Corning) in MEGM media minus the addition of bovine pituitary extract for mammosphere growth. Colonies and mammospheres were allowed to form for 8 days after which non-adherent suspension colonies from adherent culture and mammospheres from non-adherent culture were collected for analysis. Adherent colonies were fixed in methanol and stained with crystal violet for assessment of colony number (colonies > 10 cells). Colony composition was assessed by sequential immunostaining for

CK8/18 (1:500, Vector Labs) followed by DAB substrate development (Vector Labs) and CK14 (1:500, LabVision) followed by Vector VIP substrate development (Vector Labs). Stained colonies were air dried and quantified under 40X magnification.

Mammospheres collected from non-adherent culture and suspension colonies collected from adherent culture were cytospun onto glass slides and fixed in methanol for immunofluorescence analysis of CK8/18 (Vector) and CK14 (LabVison) composition with visualization by AlexaFluor-555 and Alexa Fluor-488 conjugated secondary antibodies, respectively (Invitrogen). CK14 content of mammospheres and suspension colonies was quantified by scoring the percent of the sphere that stained with CK14 with the following scale: 0 = no CK14 staining, 1 = 0-33% CK14+, 3 = 66-99% CK14+, 4 = 100% CK14+. Quantification of mammosphere and suspension colony numbers was accomplished using a Multisizer 3 COULTER COUNTER (Beckman-Coulter) that provides number, and size distributions with an overall sizing range of 14 µm to 336 µm. Suspension colonies and mammospheres were collected and pelleted at 800 rpm for 5 min and resuspended in 1ml of freshly filtered growth media. Suspension of spheres were diluted in 20 ml of 6:4 isoton II:glycerol diluent (Beckman-Coulter) and run in triplicate on the Multisizer 3.

Western blot analysis and siRNA/shRNA

Protein was extracted from cells in culture using radioimmunoprecipitation assay (RIPA) buffer supplemented with protease inhibitors. For protein stability assays, cells were treated with 30ug/mL cycloheximide (Sigma) (30min to 6 hrs) or DMSO control (6hrs) and then harvested. Protein lysates were collected at the indicated time points using RIPA buffer for Western blot analysis. Membranes were probed overnight with antibodies against SLUG (Cell Signaling), GAPDH (Chemicon), β-actin (Abcam), cyclin D1 (NeoMarkers), BARD1 (Santa Cruz), HA.11 (Covance), Dynamin (BD Bioscience) and BRCA1 (Cell Signaling). BRCA1 and BARD1 siRNA

constructs (Ambion) were transiently transfected into cells using Lipofectamine RNAiMAX following manufacturer's protocols. For immunoprecipitation experiments, 293T cells were transiently transfected with pBabe-BRCA1-HA (Addgene plasmid 14999) or pBabe-GFP. Lysates were harvested using RIPA buffer, and incubated with monoclonal anti-HA agarose beads (Sigma catalog #A2095) overnight. The beads were washed several times and lysates were eluted using 2X Sample Buffer.

SUM1315, SUM149, $BRCA1^{mut/+}$ immortalized HMECs and primary $BRCA1^{mut/+}$ cells were infected with lentiviruses for shSlug as described above. All studies with established cell lines were conducted at passage 1 following infection whereas for primary cells, 10 days after selection.

Flow cytometry and FACS

Uncultured cells from *BRCA1*$^{+/+}$ (n=10) or *BRCA1*$^{mut/+}$ (n=5) organoid preparations were dissociated to a single-cell suspension as described above and filtered through a 20 μm nylon mesh (Millipore). Endothelial, lymphocytic, monocytic, and fibroblastic lineages were depleted with antibodies to CD31, CD34 and CD45 (all Thermo/LabVision) and Fibroblast Specific Protein/IB10 (Sigma) and a cocktail of Pan-mouse IgG and IgM Dynabeads (Dynal, Invitrogen) according to the manufacturers instructions and as described previously (Villadsen et al., 2007a). Depleted single cells suspensions were resuspended at 1 x 10^6 cells/ml in phosphate-buffered saline containing 1% calf serum (FACS buffer, FB) and bound with fluorescently-conjugated antibodies to human EpCAM (APC), CD49f (PE), and CD24 (FITC) (all, BD Biosciences) for 20 min at 4C. Non-confluent cultures of SUM149, SUM1315, and immortalized HMECs cells were trypsinized into single cell suspension, counted, washed with PBS, and stained with antibodies specific for human cell CD24 (PE) and CD44 (APC) (BD Biosciences). Antibody-bound cells were washed and resuspended at 1 x 10^6 cells/ml in FB and run on a FACSCalibur flow cytometer

(BD Biosciences) or sorted on a BD Influx FACS sorter (BD Biosciences). Flow cytometry data was analyzed with the Flowjo software package (TreeStar).

Microarray hybridization and gene expression analyses

Total RNA for gene expression studies was isolated from fibroblast-depleted single cell suspensions of uncultured *BRCA1*$^{+/+}$ or *BRCA1*$^{mut/+}$ cells or from tumors generated from infected *BRCA1*$^{+/+}$ or *BRCA1*$^{mut/+}$ cells using the RNeasy Mini kit (Qiagen). Synthesis of cDNA from total RNA and hybridization/scanning of microarrays were performed with Affymetrix GeneChip products (HGU133A) as described in the GeneChip manual. Raw data files (.CEL) were converted into probe set values by RMA normalization.

Following RMA-normalization, the t-statistic ($|t| > 3.5$) was used to generate a list of genes that are differentially expressed between *BRCA1*$^{+/+}$ vs. *BRCA1*$^{mut/+}$ cells and *BRCA1*$^{+/+}$ vs. *BRCA1*$^{mut/+}$ tumors (Supplemental Tables 1 and 4, respectively). Next, hierarchical clustering was performed using the Pearson correlation metric. Prior to clustering, the expression data was filtered to include only the top 20 upregulated and 20 downregulated genes in the case of organoid analysis (Figure 3); for tumor data clustering (Figure 2), the top 50 upregulated and downregulated genes were used. Gene Set Enrichment Analysis (GSEA) was performed as described previously (Subramanian et al., 2005).

The basal gene set (Basal II) was created by sorting wild type *BRCA1*$^{+/+}$ cells with CELLection pan-mouse IgG magnetic beads according to the manufacturers instructions (Dynal, Invitrogen) conjugated to an anti-CD10 antibody (DAKO). Cells that did not bind to the CD10-immunobeads were further sorted with magnetic beads conjugated to an anti-EpCAM antibody (Abcam). RNA was extracted with the RNAeasy Mini Kit (Qiagen) from dissociated single cell suspensions of unsorted or CD10-/EpCAM+ sorted cells from *BRCA1*$^{+/+}$ qRT-PCR using an RT^2-Profiler™ custom designed (Supplemental Table 1) PCR Array following manufacturer's protocol

(SuperArray Biosciences). Ten basal genes (Basal Gene Set II) were significantly downregulated in the luminal-enriched $CD10^-/EpCAM^+$ epithelial cells compared to unsorted cells (Table S2).

Immunomagnetic Bead sorting

Epithelial organoids from $BRCA1^{+/+}$ (n=2) and $BRCA1^{+/mut}$ (n=1) patients were dissociated to a single cell suspension and sorted with CELLection pan-mouse IgG magnetic beads according to the manufacturers instructions and as described previously (Allinen et al., 2004) (Dynal, Invitrogen) conjugated to an anti-CD10 antibody (DAKO). $CD10^+$ cells were released from the beads by DNase treatment per the manufacturer's instructions. Cells that did not bind to the CD10-immunobeads were further sorted with magnetic beads conjugated to an anti-EpCAM antibody (Abcam). Positive cells were again released by DNase treatment. Viable cells from unsorted, myoepithelial enriched ($CD10^+$), luminal enriched ($CD10^-/EpCAM^+$) or depleted fractions were counted and plated for infection as described above or cytospun onto glass sides for analysis of cytokeratin expression by immunofluorescence. Cytospun cells were fixed in methanol and stained for CK14 (LabVision) and CK8/18 (Vector Labs) followed by detection with anti-rabbit or anti-mouse (respectively) fluorescently-conjugated secondary antibodies (AlexaFluor-488, Invitrogen). Immunocomplexes on the cells from immunomagnetic bead sorting were blocked with the M.O.M. Kit (Vector Labs) to allow for staining with antibodies produced in mouse (CK8/18). Positively sorted fractions were analyzed by binding a mouse secondary antibody (AlexaFluor-555 goat anti-mouse, Invitrogen) to the immunocomplexes formed from sorting for EpCAM and CD10 expression.

DiMeo & Keller et al Table S5

IHC Summary on Human Breast Tissues

Tissue #	BRCA1 status	TFF3	Vimentin
612	+/+	N/D	+
4889	+/+	+	+
625A	+/+	+++	N/D
3332	+/+	N/D	+++
8912	+/+	+++	+
12743	+/+	+	+
12522	+/+	+++	+
9402	+/+	++	+
9676	+/+	++	+
12327	+/+	+++	+
4310	+/+	++	+
2703	+/+	+	+++
618	+/+	+++	+
629	mut/+	+	++
628	mut/+	+	+++
1197	mut/+	+	+++
5185	mut/+	+	+
13408	mut/+	+	+++
3550	mut/+	+	+
49076	mut/+	+++	+++
617 (1)	mut/+	+++	+
617 (2)	mut/+	++	+++
617 (3)	mut/+	+	N/D
616	mut/+	N/D	++
627	mut/+	+	+++

$^{+}$ No to Low Lobule staining (weak staining, few positive cells (<10%) and/or few positive lobules)
$^{++}$ Moderate Lobule staining (moderate to strong staining of cells with many positive cells and/or many positive lobules)
$^{+++}$ Strong Lobule staining (Intense staining of cells with many positive cells and/or many positive lobules)
$^{N/D}$ Not determined